TRANSACTIONS OF THE INSTITUTE OF FLUID-FLOW MACHINERY

No. 130, 2015, 71–82

PAWEŁ KASZOWSKI[1] and MAREK DZIDA

CFD analysis of fluid flow through the labyrinth seal

Gdansk University of Technology, Faculty of Ocean Engineering and Ship Technology, Narutowicza 11/12, 80-950 Gdańsk, Poland

Abstract

Steam and gas turbines are essential to produce electricity. Since the launch of the first turbine in the world, there become a tendency to constantly achieve higher efficiency. There are many solutions to overcome losses in the working steam turbine. One of such methods is the use of seals. To determine thermodynamic parameters of steam, which prevail in the seal, we could use experimental methods or numerical calculations. Experimental researchs are too expensive and time consuming. Therefore, computational fluid dynamics (CFD) is increasingly used in the analysis of fluid flow through the labyrinth seal. The paper describes the results using CFD simulation software with the help of contained a computational k-ε model.

Keywords: Labyrinth seals; k-ϵ model; CFD calculations; Fliud-flow machines; Modeling

1 Introduction

Steam and gas turbines are one of the basic components in electricity producing. However, energy efficiency of turbines is not satisfactory. Since the first turbine was set in motion, the main aim of engineers is to achieve the highest efficiency as possible.

It is estimated that a reduction of 1% leakage by sealing the high-pressure part of the turbine will decrease fuel consumption by 0.4%. There are many solutions to overcome losses in the working steam turbine. One of these methods is the use

[1]Corresponding Author. E-mail address: pawkaszo1@pg.gda.pl

of seals. They can be divided into two categories – contact and clearance seals. The labyrinth seals belong to the group of clearance seals. They are used in steam and gas turbines, and other teams of turbomachines in order to separate the areas of different pressures in relatively simple but robust way. Labyrinth seals have many advantages, which include: low maintenance, simplicity of construction, reliability, high temperature resistance, relatively low impact on the destruction of the shaft, as well as wide range of the pressure difference across the seal while operating, which allows to their widespread use. But one of the major benefits of using the labyrinth seals is their long operating life, which results from their clearance form.

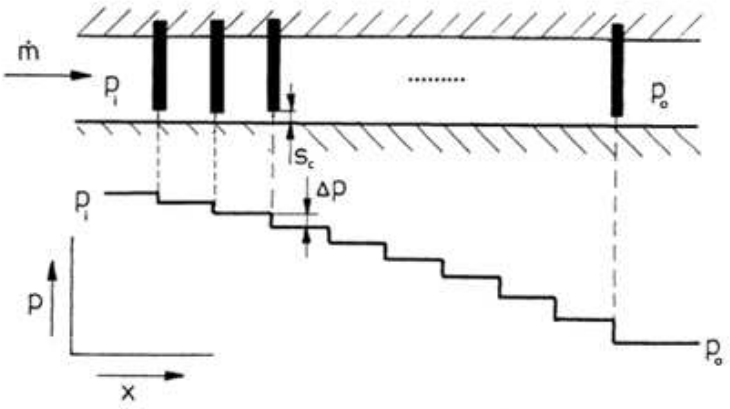

Figure 1: Scheme of the labyrinth seal without diagnostic extraction: $\dot{m}$ – mass flow, p_i – inlet pressure, p_o – outlet pressure, s_c – seal clearance, Δp – pressure drop, p – pressure, x – the lengnth of the labirynth.

Labyrinth gland consists of a serier of orifices connected with each other (Fig. 1). Because of the flow through the seal, the liquid has lost the initial value of the total pressure and at the same time it accelerated in gland slot due to the constriction of flow friction in the sealing gap and dissipation of the kinetic energy in the stuffing box. This process repeates in every slot and the seal chamber until the end thereof as it is shown in Fig. 2. Recent improvements that affect the efficiency and power gas turbines require changes in all structure components and the most important thing is reduction of leakage through the seal. Consequently, labyrinth seals are the issue, that needs more and more studies and has to be subjected to constant control also during operation of the turbine, and their configurations are still evolving. Therefore, knowledge of the exact value of the leak becomes a key information.

MOST WIEDZY Downloaded from mostwiedzy.pl

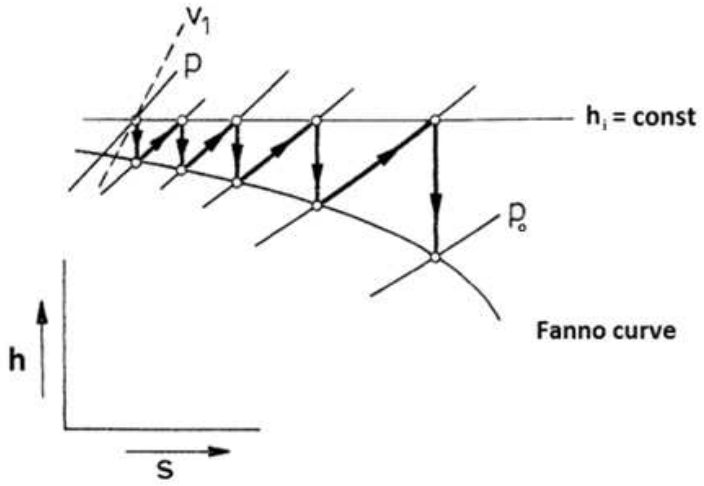

Figure 2: Fanno line for seal without extraction: v_1 – begin volume, p_i – inlet pressure, p_o – outlet pressure, h – enthalpy, s – entrpopy.

Experimental researchs are too expensive and time consuming. Therefore, computational fluid dynamics (CFD) simulations are increasingly used in the analysis of fluid flow through the labyrinth seal.

2 Model adopted to CFD calculations

Computing power of current supercomputers as well as personal computers is getting greater. It allows to perform quick numerical simulations with higher accuracy. It is an alternative for the analytical calculations. In this paper numerical calculations were performed using popular commercial CFD package FLUENT, which is one of the components of the package ANSYS Fluent software. Fluent code serves as solver to the Navier-Stokes equations using finite volume method.

A detailed description of the basis of vortex flows and turbulence modeling can be found in many standard literature items [3,8]. Turbulent flows are characterized by a variable velocity field. The transition from laminar to turbulent flow occurs when the Reynolds number, which is one of the criteria to determine the type of flow, exceeds a critical value under the dependence of the geometry which the fluid flows through. Nonlinear form of the Navier-Stokes equations, which describe the fluid flow, causes an increase in disruption in the flow in the case when the Reynolds number exceeds a critical value. This instability leads to changing in velocity field, pressure and temperature.f kinetic

MOST WIEDZY Downloaded from mostwiedzy.pl

One of the way to deal with the problem of simulation of turbulent flows are Reynolds averaged Navier-Stokes (RANS) equations, which separate the components of the velocity field on the 'medium' and 'aligning'. Direct numerical simulation (DNS), in which all length scales and time were solved, are too expensive to applied in today's computing resources. The RANS equation (where the average flow is stable) in the Cartesian coordinate system is represented by formula

$$\overline{U_k} = \overline{\frac{\partial \rho U_1}{\partial x_k}} = -\frac{\partial \overline{P}}{\partial x_i} + \mu \frac{\partial^2 \overline{U_1}}{\partial x_k \partial x_k} - \frac{\partial \overline{(\partial u_1' u_k')}}{\partial x_k} \tag{25}$$

where:

- $\overline{U_k}$ – average speeds tensor,
- $\overline{\frac{\partial \rho U_1}{\partial x_k}}$ – derivative by x variable of average speed tensor,
- $\frac{\partial \overline{P}}{\partial x_i}$ – average pressure tensor,
- μ – viscosity,
- $\frac{\partial^2 \overline{U_1}}{\partial x_k \partial x_k}$ – double derivative by x variable of average speed tensor,
- $\frac{\partial \overline{(\partial u_1' u_k')}}{\partial x_k}$ – derivative by x variable of Reynolds stress tensor.

The equations describing average flow of fluid will be solvable only if we could model the influence of the flow fluctuation on the average flow. Reynolds stress tensor in Eq. (1) is represented by element $\overline{\partial \acute{u}_1 \acute{u}_k}$. Due to the effect of fluctuation of the fluid and thermal convection, this element appears in the equation of average flow, which behaves similarly to a laminar flow of the different viscosity of the fluid between the layers. Therefore, Reynolds stress tensor can be modeled by a 'turbulent viscosity' μ_t, that is explained in

$$\overline{U_k} \frac{\partial \overline{\rho U_1}}{\partial x_k} = -\frac{\partial \overline{P}}{\partial x_i} + (\mu + \mu_t) \frac{\partial^2 \overline{U_1}}{\partial x_k \partial x_k} \,. \tag{26}$$

The k-ϵ model consists of two equations in which turbulent viscosity is expressed by energy of kinetic turbulence, κ, and energy dissipation ε:

$$\mu_t = \rho C_\mu \frac{\kappa^2}{\varepsilon} \,, \tag{27}$$

where C_μ is constant and equals 0.09.

If kinetic energy and dissipatioan are constant, component associated with fluctuations in velocity is defined as

$$\kappa = \frac{1}{2} \overline{u_1' u_1'} \,, \tag{28}$$

MOST WIEDZY Downloaded from mostwiedzy.pl

$$\varepsilon = \frac{\mu}{\rho}\overline{\Big(\frac{\partial u_1' \partial u_1'}{\partial x_k \partial x_k}\Big)}\,. \tag{29}$$

Since the equations defining in a precise κ and ε are not known, the standard k-ε model uses the following transport equation:

$$\frac{\partial(\rho\kappa)}{\partial t} + \frac{\partial(\rho\kappa u_j)}{\partial x_j} = \frac{\partial}{\partial x_j}\Big[\Big(\mu + \frac{\mu_t}{\sigma_k}\Big)\frac{\partial \kappa}{\partial x_j}\Big] + G_k + G_b - \rho\varepsilon - Y_M + S_k\,, \tag{30}$$

$$\frac{\partial(\rho\varepsilon)}{\partial t} + \frac{\partial(\rho\varepsilon u_j)}{\partial x_j} = \frac{\partial}{\partial x_j}\Big[\Big(\mu + \frac{\mu_t}{\sigma_\varepsilon}\Big)\frac{\partial \varepsilon}{\partial x_j}\Big] + C_{1\varepsilon}(G_\kappa + C_{3\varepsilon}G_b) - C_{2\varepsilon}\rho\frac{\varepsilon^2}{k} + S_\varepsilon\,, \tag{31}$$

where:

- G_k – velocity gradient forming part of the kinetic energy of turbulence defined as $2\mu_t \frac{\partial \overline{U_1}}{\partial x_j}\frac{\partial \overline{U_1}}{\partial x_j}$,
- G_b – buoyancy force,
- Y_M – fluctuations resulting from changes in turbulence,
- S_k, S_ε – the initial conditions,
- σ_k, σ_ε – experimentally designated turbulence Prandtl numbers for the kinetic energy of turbulence, equal respectively, 1.0 and 1.3,
- $C_{1\varepsilon}$, $C_{2\varepsilon}$, $C_{3\varepsilon}$ – constants experimentally determined for k-ε model, equal respectively: $C_{1\varepsilon}$=1.44, $C_{2\varepsilon}$=1.92 and $C_{3\varepsilon}$=0.09
- t – time.

The k-ε model could be only used for modeling of turbulence at a distance from the wall. Therefore, to design the behavior of fluid near the wall, as in the case of labyrinth seals, functions describing the flow near the wall averages the results.

3 Seal geometry

Geometry of the gland assumed to the calculations is presented on Fig. 3.
The calculations were performed for following parameters:

amount of sealing teeth	n:	20,
length of the seal	L:	200 mm,
hight of the orifice	h:	9.5 mm,
graduation of the seals	c:	10 mm,
width of the chamber	b:	9 m,
thickness of the orifice	d:	1.0 mm,
nominal clearance of the seals	s:	0.5 m.

MOST WIEDZY Downloaded from mostwiedzy.pl

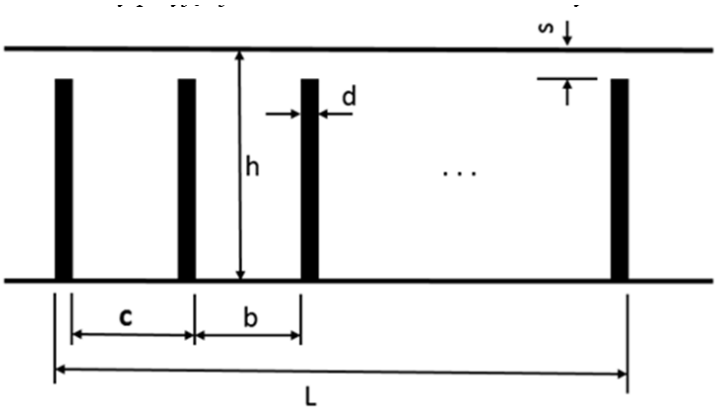

Figure 3: Geometry of gland labyrinth assumed to the calculations: b – chamber width, h – orifice height, s – nominal clearance seals, d– orifice thickness, c – seal graduation, L – seal length.

Seal geometry was modeled in Design Modeler programm included to Ansys package. Figure 4 shows the inlet channel located in the front of the seal inlet. An innovation in the geometry calculations is the application before sealing the inlet and outlet channel for the gland. Both channels are designed to stabilize the flow and have a length of 50 mm.

A grid, presented in Fig. 5, was designed in one of the programs of Mesh package. The grid consists of 1 701 931 cells and 1 713 of 993 nodes in which the calculation was made. In the sealing gaps, next its walls at a distance of 0.03 mm, the grid was concentrated to check the boundary layer. At this hight the number of grid nodes is 10.

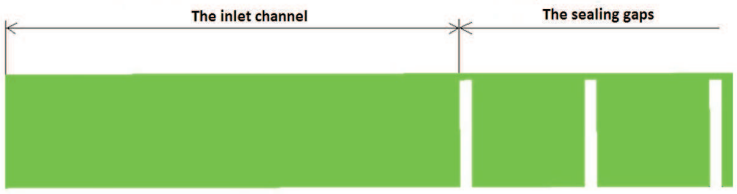

Figure 4: Fragment of gland geometry addopted to the calculation.

MOST WIEDZY Downloaded from mostwiedzy.pl

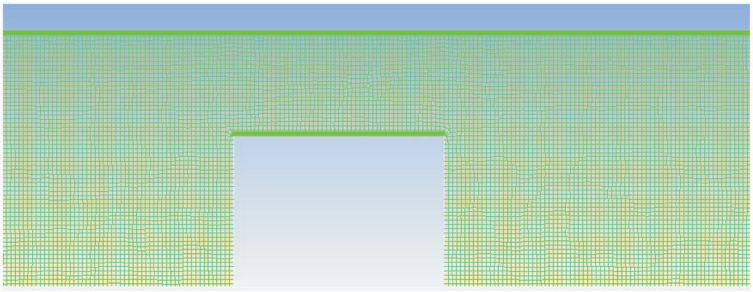

Figure 5: Computing grid for the gland labyrinth.

4 Calculations

Following boundary conditions were adopted to the calculations: pressure at the enter of inlet channel of the seal (equal to 450 000 Pa) as well as pressure at the exit of outlet channel (equal to 300 000 Pa).

The obtained results are one of the first attempts of this approach to the flow of fluid through the labyrinth gland. Similar calculations were conducted in [7] with the same boundary conditions but without modeled inlet and outlet channels.

Figure 6 presents the comparison of pressure distribution by CFD calculation both for geometry mentioned above as well as calculations made in [7] for sealing without inlet and outlet channel. In the diagram, the results obtained from numerical calculations for the gland with the inlet and outlet channel from the seal are marked by a dot, while results obtained for the sealing without channel are marked by an asterisk. There is significant difference between the two results. In the sealing without inlet channel, the pressure drop is steeper than in gland with inlet channel. In both cases, in the inlet of sealing the pressure values are the same and equal 450 000 Pa. Bigger pressure drop is noticed on the orifices of sealing in the case of the gland without the inlet channel, than in the case of sealing with the inlet channel. In both cases, the pressure difference is almost unnoticeable in the first two teeth of sealing.

Figure 7 presents the pressure drop along the length of gland. The pressure decreases in the sealing gaps and increases in gland chamber. Behind the last sealing gap, the pressure rapidly inreases (Fig. 8), as a responce of non-return valve in the outlet channel.

Thanks CFD calculations we attain the profile of pressure values in grid nodes across the width of the gap. Figure 9 represents the pressure distribution

MOST WIEDZY Downloaded from mostwiedzy.pl

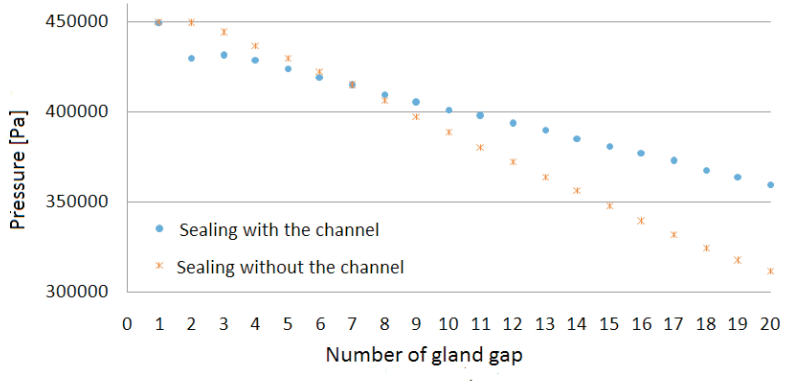

Figure 6: The comparison of pressure distribution for gland with and without the inlet channel.

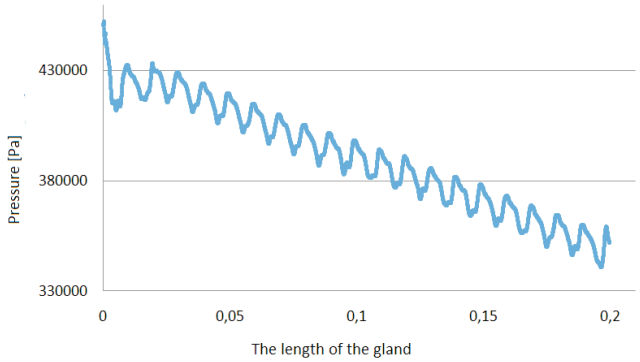

Figure 7: The pressure distribution along the length of gland with the inlet channel.

in the individual teeth of the sealing. Along the pressure values decreasing, the number of gland gap increases. From the graph it could be concluded that the maximum pressure on the profile is achieved at a height of 0.41 mm. The shape of the pressure profile is repetitive in all gaps except for the gap no. v1.

Figure 10 illustrates the comparison of fluid velocity along the length of the gland between the sealings with and without the channels, located right in the middle of gap. In the first case the velocity reached maximal values equaled 310 m/s in sealing gaps, while in the stuffing box fluid slows down to about 260 m/s. In the second case values are much smaller and reach their maximum at the penultimate gap, which is equal 117 m/s.

CFD calculations allow to visualization of phenomena occurring in the sealing. Computed maps make it possible to present the distribution of pressure and

MOST WIEDZY Downloaded from mostwiedzy.pl

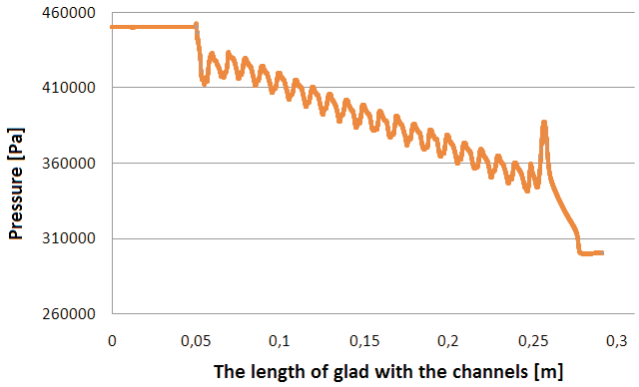

Figure 8: The pressure distribution along the sealing with the presentation of the pressure in the channels.

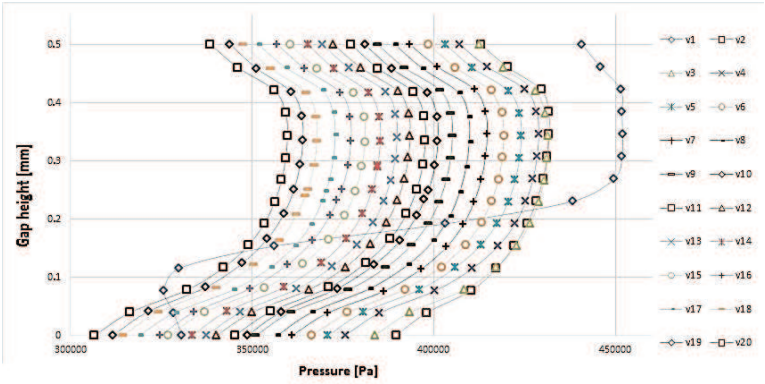

Figure 9: The pressure profile at gap height for each of sealing teeth.

velocity in such way that really affects the imagination and helps to understand and explain the results. Numerical calculations save a lot of time, which would be wasted on attain the results by the experimental method and make the experience much faster thanks possibility to set the boundary conditions already close to the expected result. Figures 11 and 12 present the visualization of results by color map mentioned above. Figure 11 shows the distribution of gas velocity both in sealing chamber and sealing gaps as well as in outlet channel, while in Fig. 12 we can see the visualization of pressure distribution.

MOST WIEDZY Downloaded from mostwiedzy.pl

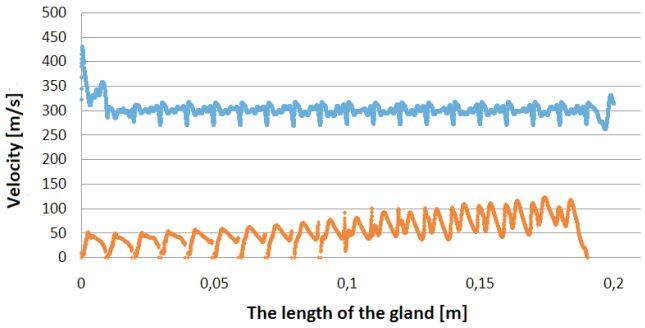

Figure 10: The graph of fluid velocity along the length of the packing.

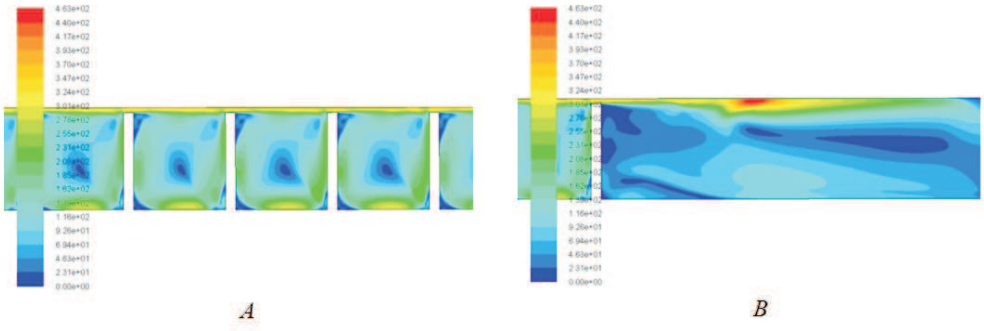

Figure 11: A) The field of gas velocity in the gaps and chambers of the labyrinth seals, B) the field of gas velocity in the outlet channel of the labyrinth seals.

5 Conclusions

The results, presented in this paper, are among the first for geometry with designed inlet and outlet channels. They are attempt to a new approach to the calculation of labyrinth glands. Further tests would show if the results are reproducible and consistent with the actual state. From the results obtained using CFD calculations, made for gland with the inlet and outlet channel in the seal, it indicates that the pressure drop in the gland with both channels is gentler. A sudden increase in pressure accurs at the outlet of the seal, which indicates that we should check what happens when we change the length of the channel. The velocity of the flow is much higher in comparison to the gland without channels.

In the literature, there are are described many computational models related

MOST WIEDZY Downloaded from mostwiedzy.pl

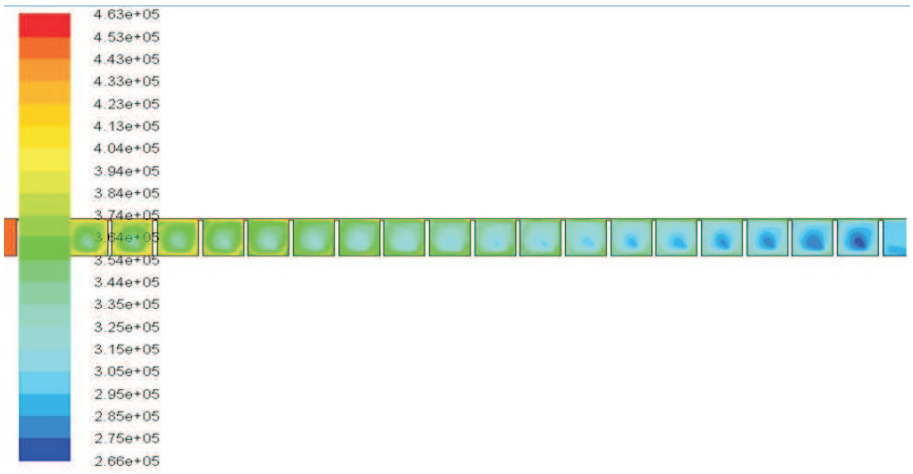

Figure 12: Pressure distribution in the labyrinth seals.

to labyrinth glands. However, analytical models do not provide much information about changes in thermodynamic parameters for the length of the labyrinth seal. Numerical calculations, especially finite element method, allow to receive the value of any parameter of the thermodynamic anywhere on seal, i.e., in the nodes of the grid.

Received 10 November 2015

References

[1] Chmielniak T.: *Thermal turbines: The theoretical basics.* Publishing House of Silesian University of Technology, Gliwice 1998 (in Polish).

[2] Eser D., Kazakia J.Y.: *Air Flow In Cavities of Labyrinth Seals.* Int. J. Eng. Sci. **33**(1995), 15, 2309–2326.

[3] Jeżowiecka-Kabsch K., Szewczyk H.: *Fluid mechanics.* Publishing House of University of Technology in Wroclaw, Wrocław 2001 (in Polish).

[4] Joachimiak D.: *Study of labyrinth seals with extraction.* PhD thesis, Poznan University of Technology, Poznan 2013.

[5] Kaszowski P.: *Analysis of labyrinth seals with extraction.* MSc thesis, Gdańsk University of Technology, Gdańsk 2014 (in Polish).

MOST WIEDZY Downloaded from mostwiedzy.pl

[6] Kaszowski P., Dzida M., Krzyślak P.: *Calculation of labyrinthseals with and without diagnostic extraction in fluid flow machines*. Pol. Marit. Res. **20**(2013), 4(80), 34–38.

[7] Kaszowski P., Dzida M.: *Comparative analysis of the result of gas flow in a labyrinth seal for a numerical and theoretical model*. J. Polish CIMAC **9**(2014), 2.

[8] 1) Kosma Z.: *Basics of fluid mechanics*. Publishing House of Kazimierz Pulaski University of Technology in Radom, Radom 2005 (in Polish).

[9] Namhyo K., Rhode D.: *Refined turbulence modeling for swirl velocity in turbomachinery seals*. Int. J. Rotating Mach. **9**(2003), 451–459.

[10] Tong K., Cha K.S.: *Comparative analysis of the influence of labyrinth seal configuration on leakage behavior*. J. Mech. Sci. Technol. **23**(2009), 2830–2838.

[11] Krzyślak P.: *A method of diagnosing labirynth seals in fluid-flow machines*. Pol. Marit. Res. **15**(2008), 3(57), 38–41, DOI:10.2478/v10012-007-0081-2.

[12] Perycz S.: *Steam and gas turbines*. Publishing House of Gdańsk University of Technology 1988 (in Polish).

[13] Piwowarski M., Kosowski K.: *Seals of thermal turbines*. Foundation for the Promotion of Shipbuilding Industry and Maritime Economy, Gdańsk 2009 (in Polish).

[14] Schramm V., Denecke J., Kim S., Wittig S.: *Shape and Optimization of a Labyrinth Seal Applying the Simulated Annealing Method*. Int. J. Rotating Mach. **10**(2004), 5, 365–371.

[15] Trütnovsky K.: *Berührungs freie Dichtungen, Grundlagen und Anwendungen der Strömung durch Spalte und Labirynthe*. VDI-Verlag Düsseldorf 1964.

[16] Wang Wei-zhe, Liu Ying-zheng, Jiang Pu-ning, Chen Han-ping: *Numerical analysis of leakage flow through two labyrinth seals*. J. Hydrodyn. B, **19**(2007), 1, 107–112.

MOST WIEDZY Downloaded from mostwiedzy.pl